Carbon Letters (2024) 34:407–420
https://doi.org/10.1007/s42823-023-00667-0

Online ISSN 2233-4998
Print ISSN 1976-4251

ORIGINAL ARTICLE

Mild purification of multiwalled carbon nanotubes with increased selectivity for carbon impurity and residual metal removal

Erdong Chen[1] · Qiang Liu[1,2] · Pan Wu[1] · Jian He[1] · Changjun Liu[1] · Wei Jiang[1]

Received: 11 October 2023 / Revised: 27 November 2023 / Accepted: 29 November 2023 / Published online: 28 December 2023

Abstract

In this study, the refinement of Multiwalled Carbon Nanotubes (MWCNTs) derived from chemical vapor decomposition is investigated. An ultrasonic pretreatment method is employed to disentangle carbon and metal impurities intertwined with MWCNTs. The pretreated MWCNTs exhibit a marginal decrease in C–O/C = O content from 8.9 to 8.8%, accompanied by a 2.5% increase in sp^3 carbon content, indicating a mildly destructive pretreatment approach. Subsequently, selective oxidation by CO_2 and hydrochloric acid etching are utilized to selectively remove carbon impurities and residual metal, respectively. The resulting yield of intact MWCNTs is approximately 85.65 wt.%, signifying a 19.91% enhancement in the one-way yield of pristine MWCNTs. Notably, the residual metal content experiences a substantial reduction from 9.95 ± 2.42 wt.% to 1.34 ± 0.06 wt.%, representing a 15.68% increase in the removal rate. These compelling findings highlight the potential of employing a mild purification process for MWCNTs production, demonstrating promising application prospects.

Keywords MWCNTs purification · Dispersion · Carbon impurities · Residual metal · Mild purification process

1 Introduction

Carbon nanotubes (CNTs) have attracted considerable interest owing to their outstanding mechanical, thermal, electrical, and structural properties [1–3]. The global demand for CNTs has increased significantly [4–6]. The catalytic decomposition of methane (CDM), as one of the typical chemical vapor deposition processes, is the most promising method for large-scale CNTs preparation. However, the purity of as-prepared CNTs (AP-CNTs) cannot be ensured because of the real-time fluctuation in the catalyst structure and the reaction conditions. The impurities are of three types: residual metal catalyst (1–10 wt.%), carbon impurities (CIs, such as amorphous carbon (AC), carbon black, graphitic fragments (GFs), and imperfections in the CNTs skeleton (such as pentagons, heptagonal carbon rings, and oxygen-containing groups). All these impurities significantly affect the CNTs properties and must be eliminated before used as a qualified product [7, 8].

Various methods have been adopted to purify the AP-CNTs [8]. The physical methods, including size exclusion chromatography, filtration, centrifugation, and high-temperature annealing, can protect the MWCNTs from damage but are usually inefficient and complex [1]. Chemical methods are more applicable, classified by liquid treatment or gas phase oxidation.

Firstly, the liquid phase treatment can typically dissolve the residual metal. A key strategy for removing the residual metal embedded in the CNTs or CIs is to damage the graphitic shells [9] or CIs and then etch the metal away using liquid oxidizers such as HNO_3, H_2SO_4, H_2O_2, or $KMnO_4$ solution or their mixtures. Although this approach can decrease the residual metal content to below 1000 ppm, the CNTs structure is inevitably damaged by the strong oxidizability, resulting in the chemical modification of the CNTs, specifically, the implantation of oxygen-containing groups on the CNTs skeleton [10, 11]. Maintaining the pristine structure of the CNTs is a crucial priority for any refinement process. Based on this goal, hydrochloric acid (HCl), a non-oxidizing acid, is an excellent choice for removing residual metal without extensive

✉ Wei Jiang
weijiang@scu.edu.cn

[1] Low-Carbon Technology and Chemical Reaction Engineering Laboratory, School of Chemical Engineering, Sichuan University, Chengdu 610065, People's Republic of China

[2] Research Institute of Tianfu New Energy, Chengdu 610065, People's Republic of China

CNTs destruction [12]. However, its effect is unsatisfactory because the metal particles are usually embedded in CIs and CNTs, making it difficult for HCl to access the metals [1, 8, 13]. Therefore, it is necessary to expose the embedded metals to HCl so that the residual metal can be removed.

Secondly, the oxidation gas (such as air/O_2 [1, 14, 15] or CO_2 [16]) oxidizes the CIs. However, it is difficult to remove CIs without excessive loss of the CNTs, owing to the highly similar chemical reactivity of the CIs and CNTs and their entanglement in AP-CNTs [8]. The oxidized rate of sp^2 carbon by CO_2 is lower than that by air/O_2 [16], which results in fewer defects. Therefore, CO_2 is considered as a better mild oxidizer than air/O_2 for removing CIs. However, the complete removal of CIs by CO_2 oxidation is difficult because CIs are located either outside or inside the CNTs skeleton. It is relatively easy to remove external CIs because they are exposed to the oxidant directly; by contrast, it is difficult to remove internal CIs because they are within the CNTs structure. Thus, Separating the internal CIs from the CNTs facilitates the purification of the AP-MWCNTs.

Based on the analysis above, the separation of residual metal, CIs from the CNTs skeleton is a priority for the AP-CNTs purification process. Ultrasonication can functionalize the surface of the CIs and the CNTs, enhancing their detachment effect [17–19]. High-energy ultrasonication is advantageous for more effective disruption of the van der Waals interaction of the CIs, residual metal with the CNTs, but it causes more severe damage to the CNTs structure. The severity of the damage is strongly affected by the dispersant [20], operating parameters of the ultrasonic device [19, 21], and natural characters of the AP-CNTs. In particular, the structural deformation of the CNTs is solvent-dependent. Less damage has been observed after sonication in water or ethanol, and high-energy ultrasonication has been found to cause more severe damage to carbon nanoparticles than to CNTs [20]. However, the current researches on ultrasonication have focused on commercial CNTs dispersion [22, 23]. The effect of ultrasonic dispersion on the CIs, residual metal, and the CNTs during the purification process has not been investigated.

Although many high-quality investigations on MWCNTs purification have been published, few were focused on the root that influence the yield and damage degree of MWCNTs. In this work, a mild three-step cascade purification process is proposed to purify the MWCNTs from the raw soot synthesized by the CCVD method. This treatment procedure mainly involves three steps: the ultrasonication of the AP-MWCNTs in ethanol to separate the CIs and residual metal, mild gas oxidation by CO_2 to eliminate the CIs, and non-oxidative etching by HCl to remove residual metal. It is found that this purification process maintains a higher yield with few defects on the pristine CNTs skeleton.

2 Experimental

2.1 Materials

Pristine AP-MWCNTs were prepared by the CDM according to the reaction process described in the Supplementary Material or in the literature [24]. First, the collected AP-MWCNTs were ground to the powder (> 200 mesh). Compressed air (21 ± 0.5 vol.% oxygen, balance nitrogen), carbon dioxide (99.2 vol.%), and nitrogen (99.999 vol.%) were purchased from Chengdu Guangdu Gas Co. Ltd. All other chemicals, including ethanol, isopropanol, methanol, HCl, HNO_3, and H_2O_2, were purchased from Chengdu KeLong Chemical Reagent Co. Ltd. and used without further purification.

2.2 Ultrasonic dispersion

AP-MWCNTs (100 mg) were placed in a 250 mL conical flask, and 100 mL of pure ethanol, isopropanol, methanol, or deionized (DI) water was added as a dispersant. The conical flask was sealed and placed in an ultrasonic cleaner (BELON10-300, Shanghai Belon Instrument Manufacturing Co. Ltd.) for 5–25 h of ultrasonication at 50–70 °C. Then the sample was filtered by a microporous hydrophobic polytetrafluoroethylene (PTFE) membrane (pore size, 0.22 μm) and then dried at 80 °C.

2.3 Etching and oxidation

AP-MWCNTs (100 mg) and 100 mL of an acid aqueous solution (5 mol·L^{-1} HCl, 5 mol·L^{-1} HNO_3, or 5 mol·L^{-1} HCl + HNO_3 at a ratio of 3:1, or 5 mol·L^{-1} HCl + H_2O_2 at a ratio of 3:1) or 100 mL of a 5 mol·L^{-1} HCl ethanol solution (named as HCl (E)) were mixed in a 250 mL conical flask, which was soaked in an oil bath with a condensation reflux device at 120 °C with continuous magnetic stirring at 300 rpm for 10 h. The sample was filtered by a PTFE membrane, washed with ethanol, and dried at 80 °C for 12 h.

The CIs in the AP-MWCNTs were selectively oxidized by CO_2. The sample was placed in a fixed-bed reactor and heated to an arbitrary temperature based on the TGA results under N_2 atmosphere. After the temperature became stable, 50 mL·min^{-1} CO_2 and 50 mL·min^{-1} N_2 were passed through the sample for 4 h, and the sample was cooled naturally to room temperature to obtain purified MWCNTs.

2.4 Mild cascade purification process

The details of CO_2 oxidation and HCl etching are listed in the SI. The MWCNTs purification steps (dispersion in

ethanol, oxidation by CO_2, and etching with HCl) were combined to construct various mild cascade purification processes, as shown in Fig. 1.

P1 was designed as a comparison experiment. In **P1-1**, AP-MWCNTs were oxidized by CO_2 at 560 °C and then etched in HCl. In **P1-2**, AP-MWCNTs were oxidized by 60 mL·min^{-1} air at 500 °C and etched in HCl. In **P1-3**, AP-MWCNTs were refluxed in HCl with subsequent CO_2 oxidation at 740 °C. In **P2**, AP-MWCNTs were ultrasonicated in ethanol for 10 h at 50 °C; they were then oxidized by CO_2 for 4 h and refluxed in HCl for 10 h. **P3** was designed to simplify the procedures of **P2**. In **P3-1**, AP-MWCNTs were refluxed in HCl (E) and oxidized by CO_2 at 640 °C. In **P3-2**, AP-MWCNTs were ultrasonicated in HCl (E) and thermally oxidized in CO_2 at 660 °C.

2.5 Characterization

Thermogravimetric analysis (TGA, STA449F3, NETZSCH) was used to determine the structural relationship among CIs, residual metal and MWCNTs. AP-MWCNTs were thermally oxidized at 30–1100 °C under 30 mL·min^{-1} CO_2 and 30 mL·min^{-1} N_2 (or 60 mL·min^{-1} air) at the constant heating rate of 5 °C·min^{-1} with/without a thermostatic during for 48 h (or 8 h) at 500 °C; The MWCNTs were examined by field-emission scanning electron microscopy (SEM, JSM7610F, JEOL Co. Ltd.) at 10 kV; Transmission electron microscopy (TEM, JEM-F200, JEOL Co. Ltd.) was used to observe the fine structure and flaws of the MWCNTs; in addition, the CIs content was evaluated at more than four random scanning positions to reduce the analytical error [25] and energy-dispersive spectroscopy (EDS) mapping was used to determine the elemental distributions; X-ray photoelectron spectroscopy (XPS, Thermo Scientific K-Alpha, Thermo Fisher) was used to determine the types of carbon in the MWCNTs; The changes in the crystallinity of the MWCNTs at 500 °C over time in air or CO_2 were recorded by in-situ Raman spectroscopy ($\lambda = 455$ nm, DXR Raman Microscope, Thermo Fisher); Ex-situ Raman spectroscopy was also used to examine the crystallinity; The zeta potentials of the MWCNTs at 25 °C were determined (Malvern Zetasizer Nano ZS90, Malvern Panalytical Ltd.) after the MWCNTs were dispersed in a mixed solution of water and alcohol at a 1:1 volume ratio; Finally, the functional groups of the MWCNTs were analyzed qualitatively by Fourier transform infrared (FT-IR) spectroscopy (Spectrum Two, PerkinElmer).

3 Results and discussion

3.1 Entanglement of AP-MWCNTs

TGA (Fig. 2A) and DTG (Fig. 2B) results confirm that the CIs and MWCNTs in AP-MWCNTs cannot be oxidized at different temperatures. First, the temperature at which AP-MWCNTs mass loss began in CO_2 (550 °C) was higher than that in air (475 °C), because CO_2 is a weaker oxidizer [16]. Secondly, the residual mass ratios [25] were 9.95 ± 2.42 wt.% in CO_2 and 10.47 ± 2.56 wt.% in air, with deviations that cannot be eliminated by either oxidant [12, 14]. Finally, two wide oxidation peaks appear in the CO_2 derivative thermogravimetry (DTG) curve. The peak at 779 °C represents the oxidation of AC and some CNTs, and that at 978 °C is attributed to the oxidation of MWCNTs and GFs, owing to the common oxidation sequence of the AC, single-walled CNTs, MWCNTs, and GFs [26, 27]. These results are consistent with those of the standard carbon samples (Fig.S1). By contrast, the air-DTG curve shows only a single wide oxidation peak at 450–720 °C, which can be also divide into two peaks at 613 °C and 644 °C, representing the oxidation of AC/CNTs and MWCNTs/GFs, respectively.

In addition, the results of thermostatic TGA and in-situ Raman spectroscopy also show that the CIs and CNTs cannot be oxidized separately completely. Although approximately 80 wt.% of the AP-MWCNTs has been oxidized

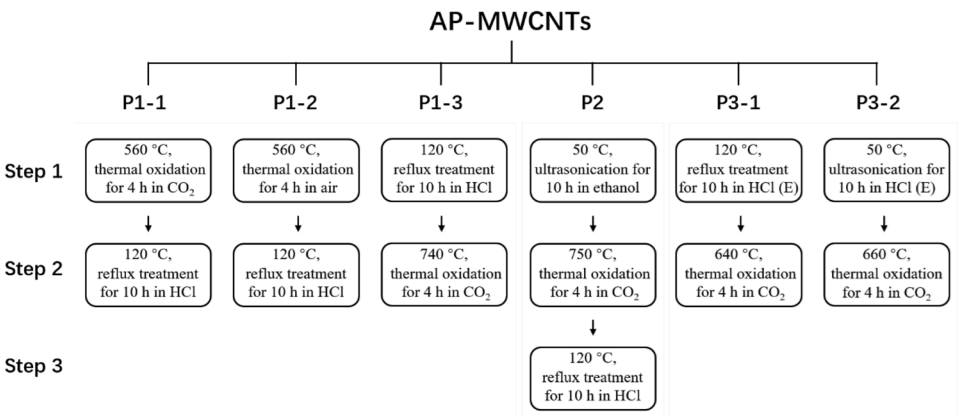

Fig. 1 Descriptions of mild cascade purification processes

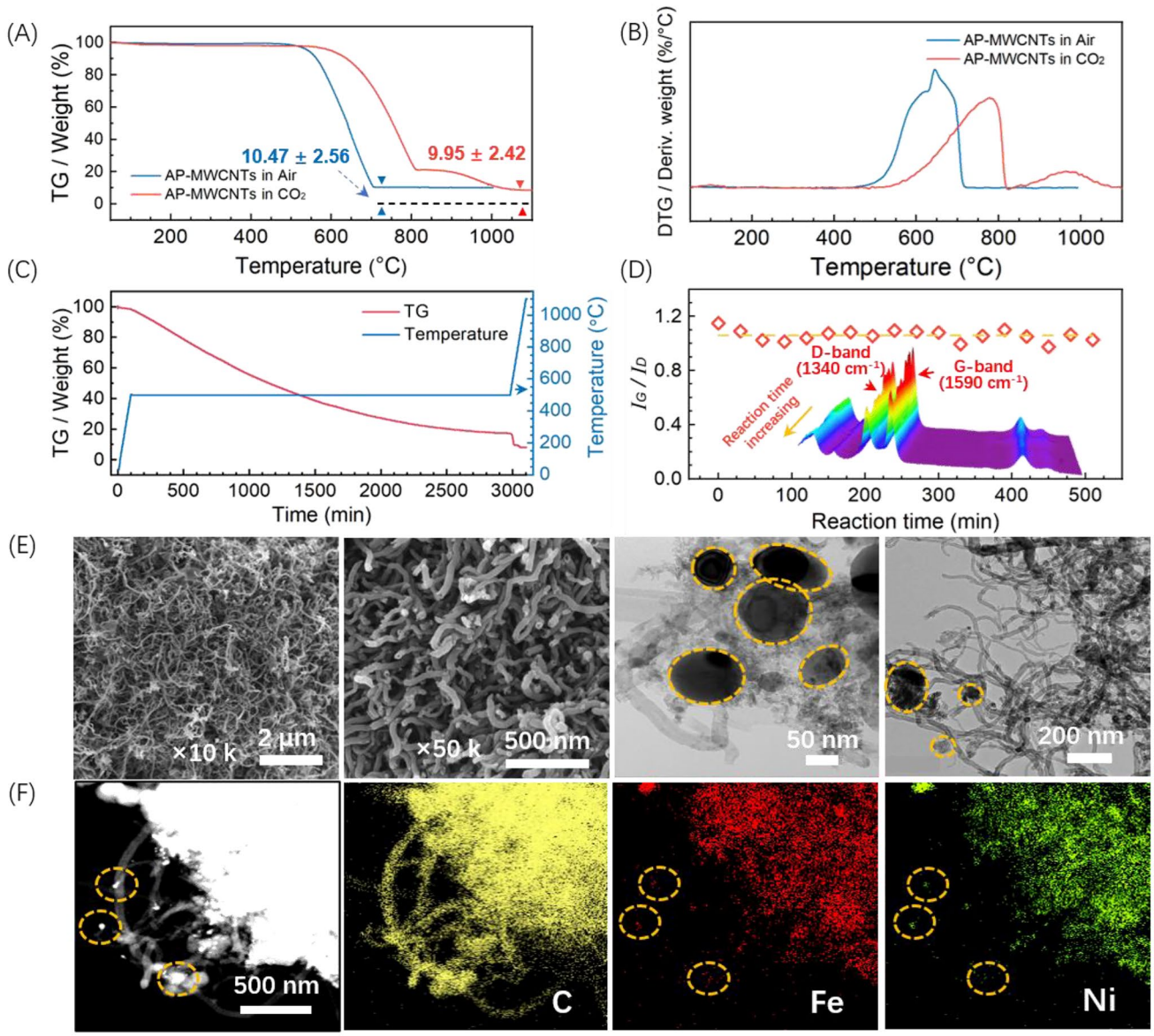

Fig. 2 Characteristics of AP-MWCNTs: **A** TGA results, **B** DTG results, **C** TGA at 30 mL·min^{-1} CO_2 and 30 mL·min^{-1} N_2, 5 °C·min^{-1}, 30–1100 °C followed by 48 h at 500 °C, **D** In-situ Raman results with temperature held at 500 °C for 500 min in CO_2, **E** SEM and TEM images, **F** EDS mapping images

when the temperature was held at 500 °C for 48 h (in CO_2, Fig. 2C), no separate stage is observed. Moreover, the in-situ Raman results (Fig. 2D) also show that the oxidation behavior of the AP-MWCNTs in CO_2 or in air did not differ greatly excepting that the oxidation rate was relatively low in CO_2. The D-band peak at 1335–1345 cm^{-1} is ascribed to morphological defects in the CNTs caused by the symmetry breakdown of carbon atoms close to the edges of graphite sheets [28]. The G band at 1590 cm^{-1} is assigned to the sp^2-hybridized carbon networks in ordered graphite [29]. Regardless of the oxidizer, the area ratio of these two bands (I_G/I_D) is almost the same, 1.1.

SEM, TEM and EDS-mapping images confirm that the CIs and MWCNTs in AP-MWCNTs are highly entangled and interwoven. Compared to fresh catalyst (Fig. 5A), SEM images (Fig. 2E) of AP-MWCNTs represent that a large amount of carbon nanofibers accumulate on the catalyst, and few CIs cover on their skeletons. TEM images (Fig. 2E) demonstrate that they are MWCNTs with a wide estimated diameter range of 5–60 nm (Fig.S1), resulting in a wide oxidation temperature range [26, 27]. Furthermore, the corresponding EDS mapping images (Fig. 2F) indicate that the aggregations in the AP-MWCNTs are the combination of carbon (AC, CNTs, or GFs) and residual

metal (Fe, Ni), but residual metal also appears inside the MWCNTs.

The results above confirm that the oxidation temperatures of different carbon allotropes cannot be clearly distinguished dynamically, although their CO_2 oxidation thermodynamics differ (Fig. 2B). The rationale is the very poor gas–solid diffusion owing to the interweaving of CIs and CNTs, which hinders gas diffusion to the CIs. It is common that AP-MWCNTs synthesized by catalytic chemical vapor decomposition (CCVD) have a state of entanglement and interweaving among CIs, residual metals and CNTs [30]. Thus, overcoming the limited mass transfer is a crucial task in AP-MWCNTs purification.

3.2 Dispersion of AP-MWCNTs

Methanol, ethanol, and isopropanol were used as the dispersants to separate CIs, residual metal, and CNTs in the AP-MWCNTs prior to CO_2 oxidation, with DI water serving as a control. The temperatures at which rapid weight loss occurs (Fig. 3A and Table 1) in the treated AP-MWCNTs increase to approximately 790–837 °C from only 534 °C. This confirms the separation of residual metal from carbon and the removal of CIs from the CNT skeleton [8, 31], which greatly decreases the mass transfer resistance of CO_2 in oxidation. Such effective purification of CNTs by ultrasonic operation is in agreement with the results reported, removing catalysts and graphitic particles adhered to single-walled CNTs [32], and separating the amorphous carbon enwrapped inside CNTs [33]. However, the multi-walled structure of AP-MWCNTs increases the difficulty of removing impurities and requires higher ultrasonic intensity and longer treatment time, which could lead to a significant increase in the damaging risk of CIs structure [34]. Thus, a suitable solvent condition for ultrasonic treatment of AP-MWCNTs is important.

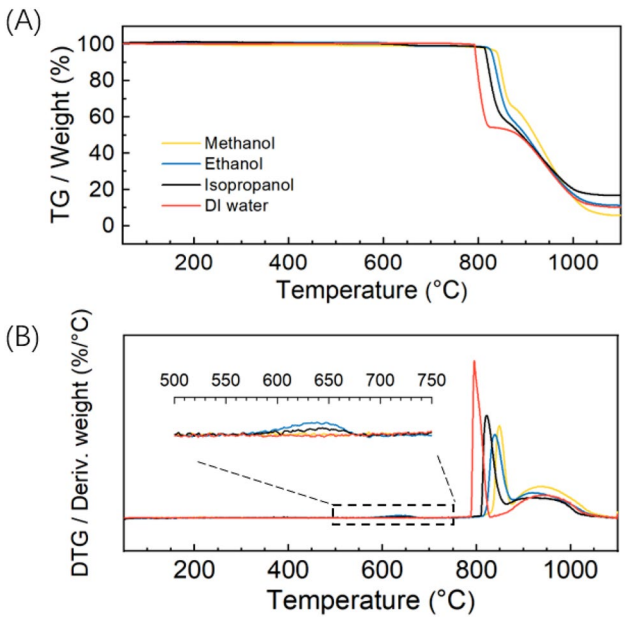

Fig. 3 AP-MWCNTs after ultrasonication for 10 h at 50 °C: results of (**A**) TGA and (**B**) DTG in CO_2

Table 1 TGA and DTG results summary of initiation, oxidation temperature after different treatment

Sample	Initiation Temperature (°C)	Oxidation Temperature (°C)		
		Peak1	Peak2	Peak3
AP-MWCNTs	534	–	779	978
Methanol	570	639	850	938
Ethanol	570	639	839	922
Isopropanol	570	639	822	937
DI Water	785	–	796	942
50 °C for 5 h	548	662	860	923
50 °C for 10 h	548	637	840	923
50 °C for 15 h	548	637	854	923
50 °C for 20 h	548	637	819	923
50 °C for 25 h	548	637	853	923
60 °C for 5 h	525	681	872	931
60 °C for 10 h	525	639	825	938
60 °C for 15 h	525	639	829	930
60 °C for 20 h	525	687	–	936
60 °C for 25 h	525	678	870	930
70 °C for 5 h	530	691	–	949
70 °C for 10 h	530	700	–	949
70 °C for 15 h	530	707	–	936
70 °C for 20 h	530	695	–	936
70 °C for 25 h	530	711	–	934

A new peak appears at 639 °C in the DTG curves of AP-MWCNTs after ultrasonication (Fig. 3B). This heat release should originate from the oxidation of AC released from the CNT skeleton by the combined action of ultrasonication and each dispersant. However, when water was used as the dispersant, the linkage between AC and CNTs was not broken owing to the hydrophobicity of AP-MWCNTs [35]. Thus, water cannot easily enter the pores in the primary agglomerates in the AP-MWCNTs and come into closer contact with carbon to separate the AC from the CNTs under ultrasonication [36].

The second oxidation peak, which is attributed mainly to MWCNT oxidation, increased by approximately 60 °C compared with that of the untreated AP-MWCNTs, indicating a sharp increase in the purity of the MWCNTs (Table 1). The reason is that ultrasonication detaches AC and residual metal from the MWCNT skeletons [25], causing this DTG peak to become sharper owing to the relatively pure carbon content [26, 27]. The third peak, which is ascribed to the mixture of

MWCNTs and GFs, remains the same in all cases, suggesting that ultrasonication cannot separate them.

Thus, it can be concluded that ultrasonication in alcohols can effectively separate CIs and residual metal from MWCNTs, improving the effectiveness of the oxidation process for AP-MWCNT purification. Alcohols are necessary during ultrasonication as a dispersant to decrease the hydrophobicity of MWCNTs. In the experiments described below, ethanol is used as the dispersant.

The effect of operating temperature and duration of ultrasonication in ethanol was investigated, as shown in Fig. 4A. After ultrasonication at 50 °C, the temperature at which oxidation began increased to 800–838 °C for most MWCNT samples, except for that after 5 h of treatment. However, three separate DTG peaks were observed for all samples regardless of the duration of ultrasonication (Fig. 4B and Table 1). The mass loss of the sample treated for 5 h in the low-temperature zone (548–700 °C) was 15.5 wt.%, which is much larger than those of the other samples (approximately 3.0 wt.%), and its oxidation peak was 25 °C higher. This first peak is attributed to a mixture of AC and MWCNTs with small diameters or many defects [24, 25] because CIs cannot be adequately separated by a short period of ultrasonication. Extending the ultrasonication time facilitates the complete separation of CIs from MWCNTs and thus results in sharp discrete peaks.

When the ultrasonication temperature is increased to 70 °C, MWCNTs are destroyed regardless of the duration. Samples ultrasonicated for different durations all begin to exhibit rapid mass loss at approximately 600 °C (Fig. 4C), and the DTG peak of MWCNTs disappears (Fig. 4D and Table 1). This notable change is ascribed to the strong destructive effect of ultrasonication at high temperatures, which breaks the MWCNTs and generates many highly defective MWCNTs and even carbon fragments (see the TEM images in **Fig.S2**), which can be oxidized at lower temperatures. It can be concluded that the ultrasonication of MWCNT at 70 °C is highly destructive.

Therefore, an intermediate temperature of 60 °C was adopted; the TGA results in Fig. 4E show an intervening

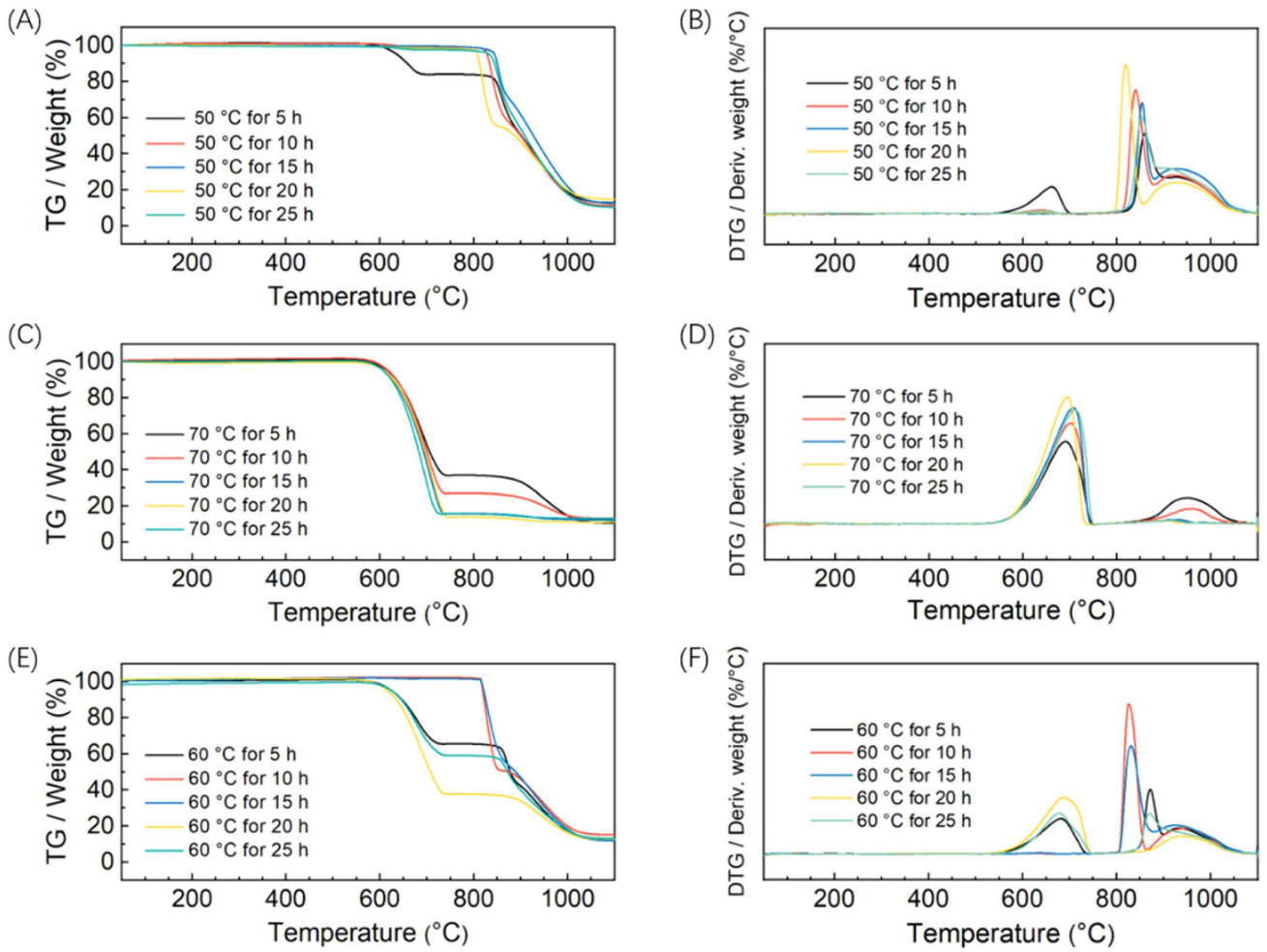

Fig. 4 TGA and DTG results of AP-MWCNTs in CO_2 after ultrasonication in ethanol for 5–25 h at (**A**, **B**) 50 °C, (**C**, **D**) 70 °C, (**E**, **F**) 60 °C

regularity partly similar to both cases. The results obtained at 50 °C and 70 °C indicate that a short treatment did not fully remove the initial CIs, but high temperature and long duration damaged the MWCNTs. A treatment time between 10 and 15 h is thus considered suitable for removing CIs without destroying the MWCNT skeleton at 60 °C. The DTG results in Fig. 4F and Table 1 confirm this result, because only two main isolated peaks, at 827 °C for the MWCNTs and at 934 °C for GFs, appear after 10 and 15 h of ultrasonication.

Thus, it can be concluded that the treatment temperature is a decisive factor affecting MWCNT damage, and a long treatment time is suitable for CI separation. After AP-MWCNTs were treated at 50 °C for more than 10 h or at 60 °C for 10 to 15 h, the desired separation of CIs and MWCNTs can be achieved, in preparation for oxidation in CO_2 to obtain qualified MWCNTs.

The structure of AP-MWCNTs before and after ultrasonication was observed by SEM. As shown in Fig. 5A–C, many CNTs grew densely on the catalyst surface, and entangled CNTs completely covered the surface [37] After 10 h of ultrasonication at 50 °C, the compact entanglement was maintained, and more CIs (yellow circles) appeared on the CNT surface (Fig. 5D). However, when the ultrasonication time was extended to 25 h, the MWCNT aggregations were looser, and fewer exposed CIs adhered to the surface, suggesting that impurities were successfully separated (Fig. 5E). When the temperature was increased to 60 °C (Fig. 5F and Fig. 5G) or 70 °C (Fig. 5H and Fig. 5I) the CNTs were partially or completely stripped from the aggregations. However, no destruction of MWCNTs is observed owing to the limitations of SEM. The SEM observations visually indicate that ultrasonication loosened the AP-MWCNT aggregations and exposed CIs.

Qualitative analysis by FT-IR spectroscopy (Fig. 6A) shows that ultrasonication had no notable effect on AP-MWCNTs, excluding sp^3 carbon [38]. For the sample ultrasonicated for 25 h at 50 °C, the peak at 1386 cm^{-1}, which is attributed to the bending vibration of $–CH_3$ [2], is enhanced, and that at 1397 cm^{-1}, which is attributed to –C–H– deformation [39], is weakened, indicating that the sp^3 carbon content increased and the sp^2 carbon content decreased. Moreover, the C–OH peak at 1050 cm^{-1} and C–O peak at 1160 cm^{-1} are weak, and the –COOH peak at 1740 cm^{-1} is negligible [16], demonstrating that ultrasonication had little effect on the generation of oxygen-containing groups.

The XPS spectrum also confirms that few MWCNTs were destroyed by ultrasonication. As shown in Fig. 6B, the C 1 s peak can be deconvoluted into three peaks at 284.8, 285.5, and 286.5–288.0 eV, which are assigned to sp^2 carbons, sp^3 carbons, and C–O/C = O, respectively [38]. A perfect CNT skeleton contains only sp^2 carbon. However, after ultrasonication in ethanol at 50 °C for 25 h, the sp^3 carbon content increased from 13.8% to 16.3%, and the C–O/C = O content decreased slightly, from 8.9% to 8.8%. By contrast, the sp^3 carbon content increased to 16.3% (60 °C for 25 h) and 18.3% (70 °C for 25 h), and C–O/C = O increased sharply to 12.6% (60 °C for 25 h) and 16.7% (70 °C for 25 h). These results confirm that ultrasonication strongly affected the conversion of sp^2 carbon to sp^3 carbon.

The Raman spectrum (Fig.S3) shows that R (I_G/I_D) increases from 1.26 (AP-MWCNTs) to 1.36 (after

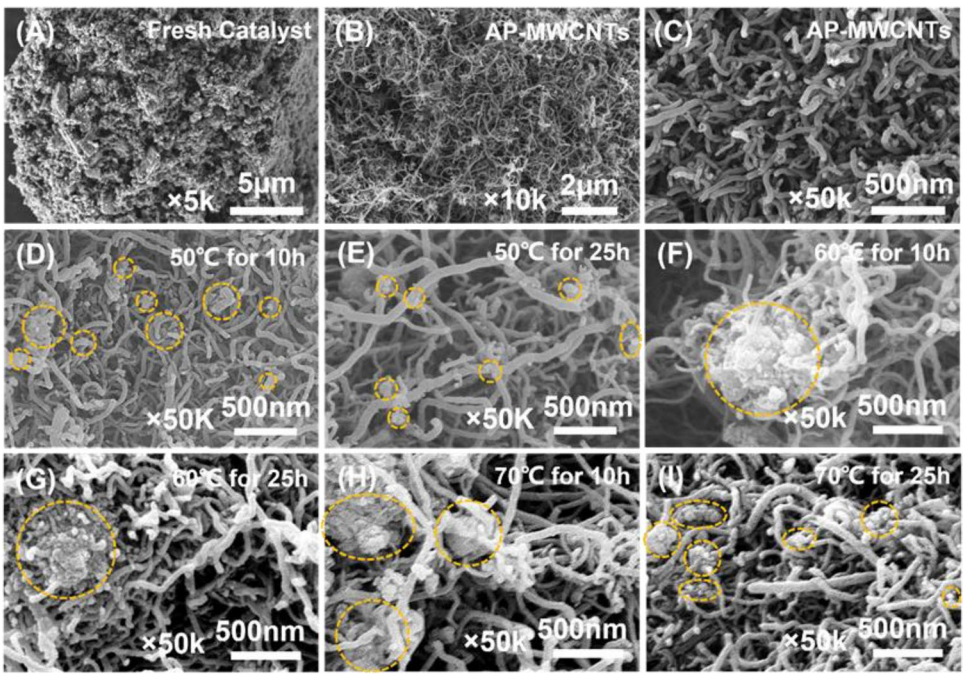

Fig. 5 SEM images of (**A**) fresh catalyst, (**B**, **C**) AP-MWCNTs, and AP-MWCNTs after ultrasonication at (**D**) 50 °C for 10 h, (**E**) 50 °C for 25 h, (**F**) 60 °C for 10 h, (**G**) 60 °C for 25 h, (**H**) 70 °C for 10 h, and (**H**) 70 °C for 25 h

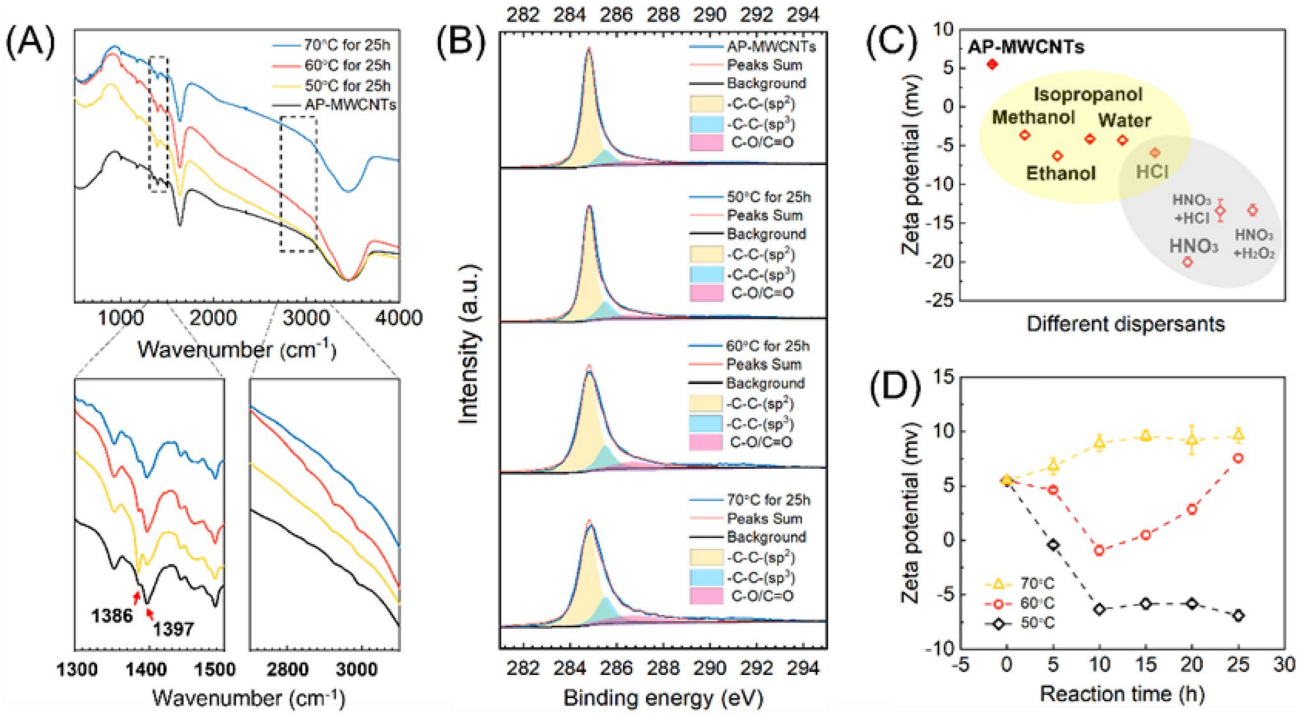

Fig. 6 **A** FT-IR spectra, (**B**) C 1 s XPS spectra, and (**C**, **D**) zeta potentials of AP-MWCNTs before and after ultrasonication

ultrasonication at 50 °C for 25 h), 1.35 (after ultrasonication at 60 °C for 25 h), and 1.46 (after ultrasonication at 70 °C for 25 h). The enhanced graphite degree indicates the removal of CIs.

The zeta potentials show that surface electrification breaks the van der Waals force between CIs and CNTs. As shown in Fig. 6C, the zeta potential decreased from 5.52 ± 0.09 mV (AP-MWCNTs) to -3.62 ± 0.10 mV (in methanol), -6.32 ± 0.38 mV (in ethanol), -4.12 ± 0.24 mV (in isopropanol), and -4.26 ± 0.35 mV (in water) after ultrasonication at 50 °C for 10 h. When the AP-MWCNTs were dispersed in ethanol, the zeta potential decreased to approximately − 6.0 mV after ultrasonication at 50 °C, but it increased to 9.0 mV after ultrasonication at 70 °C (Fig. 6D).

The level of the zeta potential is not only related to the amount of surface charge but also to the distribution position of surface charge [14]. The zeta potential is positive at 70 °C because the positive and negative charges are distributed in the vacancy position, resulting in more positive C exposed than negative O, so the overall external positive charge. The surface damage at 60 °C is less than that at 70 °C, but there is also damage leading to external charge instability. At 50 °C, the surface is basically not damaged, so that C exists inside and O is outside, resulting in an external negative charge.

These changes are attributed to less ionization of –COOH or –OH groups owing to the acceleration of the hydrolysis reaction at high temperatures [40]. In addition, during ultrasonication at 60 °C, the zeta potential first decreased and t hen increased, confirming that CIs were first removed to expose the MWCNT surface, and then the MWCNT skeleton was destroyed.

The above analysis indicates that the ultrasonication of AP-MWCNTs in ethanol can separate CIs from MWCNTs, but it damaged the MWCNT skeleton to some extent. The ultrasonication temperature is a decisive factor affecting the damage to MWCNTs, and a longer duration can worsen the damage but enhance the dispersion degree.

3.3 Selectivity of gas oxidation and liquid etching

After ultrasonic treatment, the residue CIs and metal impurities originated from catalysts remained in AP-MWCNTs should be further removed for quality improvement. For CIs removing, three possible gases, CO_2, O_2 and H_2, are compared for determining the feasibility based on the selectivity simulation on different carbon allotropes at the thermodynamic level.

As shown in Fig. 7A, the conversion rate of graphite carbon (GC) by O_2 always pertains 100% in the whole temperature range from 0 to 1200 ℃, indicating its excessive strong oxidizability without enough space for selective tuning, achieving CIs removal. However, H_2 can completely reduce GC to methane below 200 ℃ and partially reduce below 800

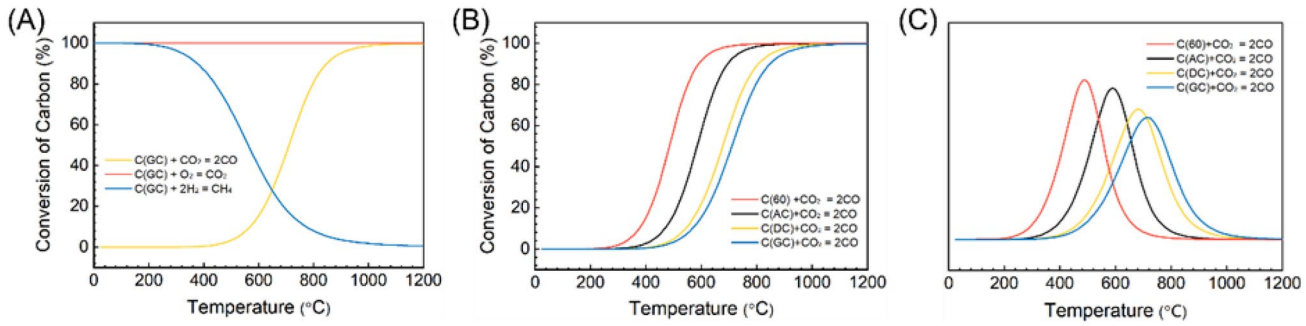

Fig. 7 **A** Thermodynamic equilibrium of graphitic carbon oxidation in O_2, CO_2 and H_2; **B** Thermodynamic equilibrium of carbon allotropes oxidation in CO_2; **C** Derivative results of CO_2 oxidation thermodynamic equilibrium of carbon allotropes

ºC, and CO_2 can partially oxidize GC to CO below 1000 ºC and achieve complete oxidization after beyond this temperature point. This simulation confirms that CO_2 is a relatively mild oxidizer and can be used partially removing CIs from AP-MWCNTs if the temperature raising sufficiently.

Investigating the thermodynamic equilibrium conversion rate of four main carbon allotropes contained in AP-MWCNTs, including GC, C_{60}, AC, and $C_{diamond}$, reacting with CO_2, a significant difference among four species can be observed (Fig. 7B and C). It can be determined that GC is the most difficult to be oxidized by CO_2 with the highest starting temperature of the reaction. The peak positions of conversion rate after derivation of C_{60}, AC, $C_{diamond}$, and GC, are 484 ºC, 595 ºC, 684 ºC, and 713 ºC, respectively. This occurrence exhibits a thermodynamic feasibility by using CO_2 as the oxidizer to selectively remove CIs since the least temperature gap of oxidization with CO_2, between DC and GC, has reached 29 ºC. However, the actual removal effect of CIs by CO_2 oxidization should be testified and evaluated due to the aggregation status of different carbon species in AP-MWCNTs which evokes strong mass transfer resistant and converts the process into kinetical controlling. Ultrasonic dispersion is necessary to expose CIs, reducing the negative effect of aggregation and promoting the purification according to thermodynamic.

The removal of metal impurities of MWCNTs usually is acid etching [1]. Four etching liquid is used for achieving this purpose, including HCl, HNO_3, HCl + HNO_3, and HCl + H_2O_2. The TEM images of the acid-treated samples shown in Fig. 8 confirms the different removing the effect of the etching solution, including the metal particle residual amount and structure destruction degree of MWCNTs. The residual metal of the sample treated by HCl is the most, but no observable damage of MWCNTs is detected, which is

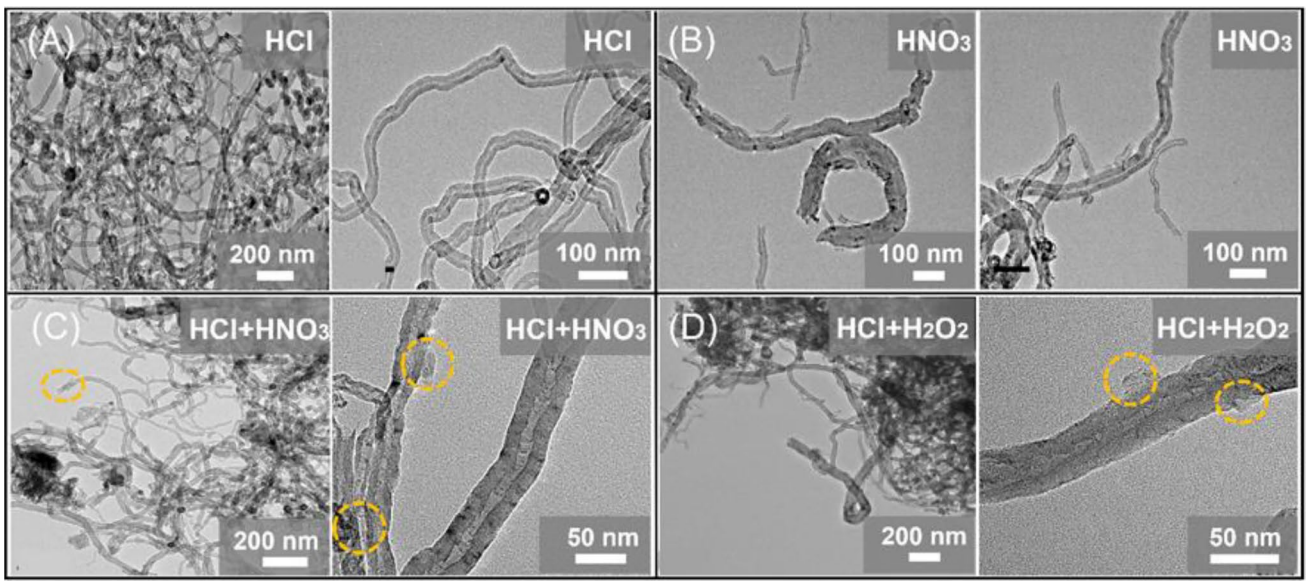

Fig. 8 TEM images of AP-MWCNTs treated in acid: **A** HCl; **B** HNO_3; **C** HCl + HNO_3; **D** HCl + H_2O_2

ascribed to the non-oxidizability of HCl [41, 42]. However, HNO_3 can effectively eliminate residual metal, but severely damages the main structure of MWCNTs simultaneously due to strong oxidizability [43]. Using a hybrid solution of HCl and HNO_3, the metal remove the effect and MWCNT structure damaging is intermediate between the former two. Some metal embedded in MWCNTs and CIs on tube walls fail to remove although the perfection of MWCNTs structure is basically maintained in treatment. The effect of $HCl + H_2O_2$ is similar to $HCl + HNO_3$ [44].

Therefore, the post-treatment procedures for purifying AP-MWCNTs after ultrasonic treatment are determined to be gas oxidation by CO_2 for eliminating CIs due to its mild oxidizability and usable selectivity, and liquid etching by HCl for dissolving metal impurities due to its least damage effect of MWCNTs structure.

3.4 Mild purification process

In the **P1** process, ultrasonic dispersion in ethanol is omitted, and oxidation in CO_2 or air and acidification with HCl are applied. As shown in Table 2, the total MWCNT yields of all three processes are relatively low: 65.74 wt.% for **P1-1**, 60.86 wt.% for **P1-2**, and 76.49 wt.% for **P1-3**. The metal content after treatment is high: 2.90 ± 0.68 wt.% for **P1-1**, 2.61 ± 0.67 wt.% for **P1-2**, and 1.93 ± 1.45 wt.% for **P1-3**.

TEM images confirm that the **P1** processes (**P1-1**, **P1-2**, and **P1-3**) cannot simultaneously ensure the structural integrity of the MWCNTs at a high yield and a high CI removal rate. The **P1-1** process caused little damage, because CO_2 is a weak oxidant, and HCl is a non-oxidative acid, but many CIs remained interwoven with MWCNTs (Fig. 9A and **Fig. S7A**). When air was used instead of CO_2 (**P1-2**), the damage to MWCNTs was more severe, although most of the CIs were removed (**Fig.S9B** and **Fig.S7B**) owing to the strong oxidation capacity of air in the first step, and this process had the lowest yield, 71.22 wt.%. When the order of the two steps of **P1-1** was reversed, in **P1-3**, the obtained MWCNTs exhibited greater structural integrity than those obtained using **P1-2**, but less structural integrity than those obtained using **P1-1**. The CI removal rate (**Fig.S9C** and **Fig.S7C**) was also intermediate between those of **P1-1** and **P1-2**.

The **P2** process has an attractive yield and CI/residual metal removal rates. No weight loss occurred in the ultrasonic dispersion step, and 94.33% and 90.80% of the weight was retained during oxidation and etching; these values are much larger than those of the other processes. The total MWCNT yield was 85.65 wt.%, and only 1.34 ± 0.06 wt.% remained as residual metal (Tab.2). This significant improvement is ascribed to the excellent dispersion effect of ultrasonication, which increases the selectivity of CO_2 oxidation for CIs, and the accessibility to HCl of residual metal inside MWCNTs or CIs. The TEM images in Fig. 9D and **Fig.S8** show that the MWCNTs are highly dispersed and show the least damage and lowest CI and residual metal contents, indicating that the three-step process exhibits excellent purification performance.

P3 did not perform as well as **P2** but outperformed any **P1** process. The total MWCNT yield of **P3-1** was 86.15 wt.%, and that of **P3-2** was 88.62 wt.%; the residual metal contents were 1.72 ± 0.22 wt.% and 5.77 ± 0.20 wt.%, respectively (Table 2). The total yield in both cases was slightly higher than that of **P2**, but the MWCNTs were significantly more degraded (Fig. 9E**,** F**,** and **Fig.S9**). The MWCNTs purified by **P3-1** had excessive defects, and those purified by **P3-2** contained many CIs inside MWCNTs.

The Raman results in Fig. 10A and **Fig.S10** show that all the R ($=I_G/I_D$) values are higher than that of the AP-MWCNTs (1.26), except for that of the MWCNTs purified by **P3-1**, which suggests that their crystallinity and graphitization degrees were higher after purification. The R value of each step varies depending on the trade-off between CI removal and MWCNT damage, but the overall improvement indicates effective purification. Typically, the R value of the **P2** process increases from 1.26 to 1.34 after ultrasonication owing to the removal of CIs, but it decreases slightly (to 1.33) after CO_2 oxidation and decreases further (to 1.29) after refluxing in HCl owing to the mildly damaging effect of the latter two steps.

Furthermore, the XPS results (Fig. 10B and **Fig.S11**) confirm that the C–O/C = O content of MWCNTS purified by **P2** is lower (16.9%) than that of MWCNTs purified by the other processes, although it is higher than that of pristine AP-MWCNTs (8.9%). The MWCNTs purified by **P1-2** have the highest C–O/C = O content (21.6%) because of the strong oxidation capacity of air. The next-highest C–O/C = O contents were found in the MWCNTs purified by **P3-1** (17.7%) and **P3-2** (18.7%) owing to the combined effects of ethanol and HCl. It is interesting that the sp^3 carbon content of MWCNTs purified by **P2** decreased slightly (by 0.8%), whereas those of MWCNTs purified by the other processes increased (to 14.9% for **P1-1**, 14.9% for **P1-2**, 15.9% for **P1-3**, 18.9% for **P3-1**, and 18.5% of **P3-2**, from 13.8% for

Table 2 Yields of each purification process

Process	MWCNT yield (wt.%)				Residual metal (wt.%)
	Step 1	Step 2	Step 3	Total	
P1-1	78.26	84.00	–	65.74	2.90 ± 0.68
P1-2	71.22	85.44	–	60.85	2.61 ± 0.67
P1-3	82.67	92.53	–	76.49	1.93 ± 1.45
P2	100.00	94.33	90.80	85.65	1.34 ± 0.06
P3-1	88.87	97.13	–	86.15	1.72 ± 0.22
P3-2	93.06	95.23	–	88.62	5.77 ± 0.20

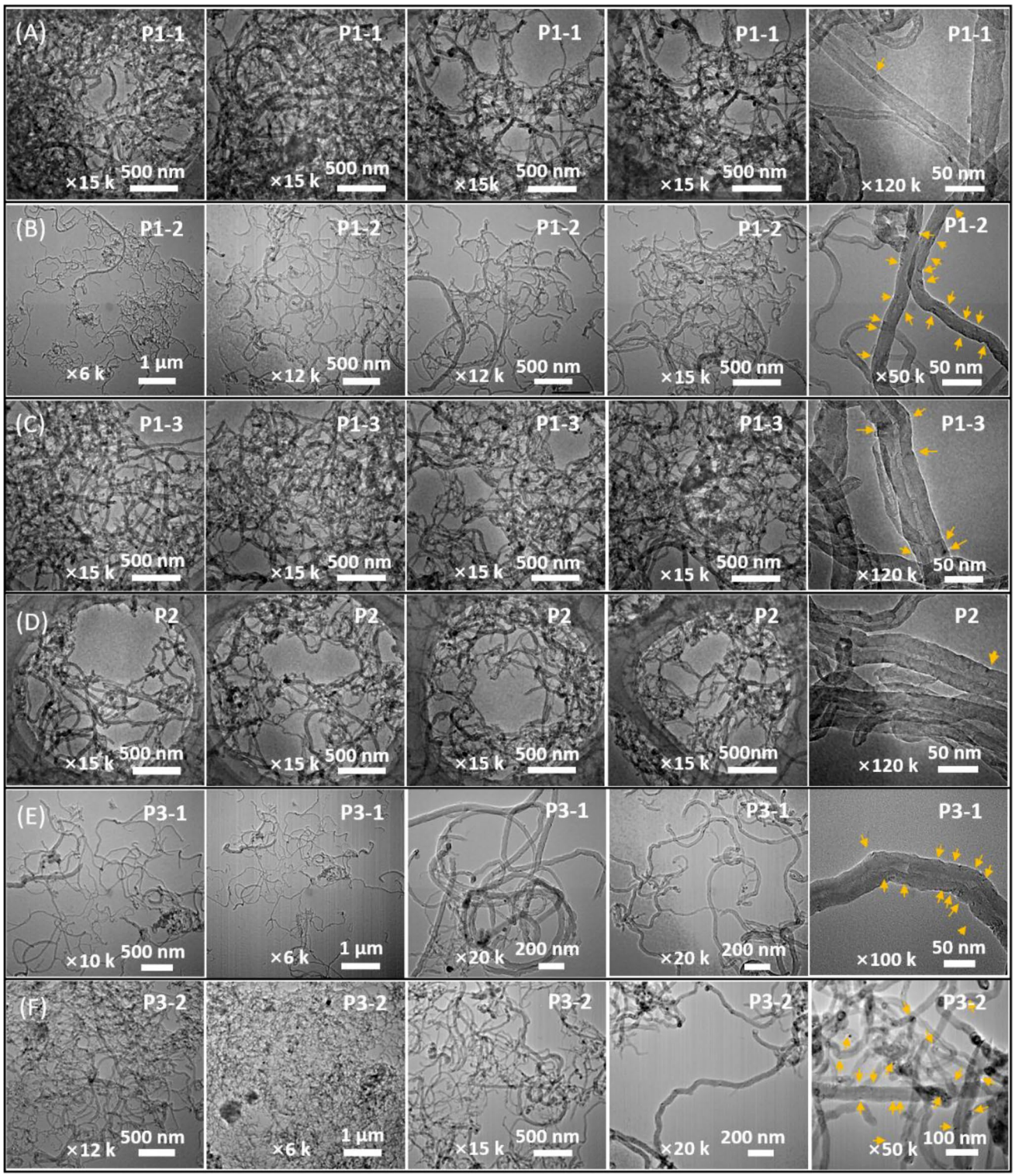

Fig. 9 Products TEM images of **A** P1-1, **B** P1-2, **C** P1-3, **D** P2, **E** P3-1, and **F** P3-2

pristine AP-MWCNTs). The results of the **P2** process demonstrate that ultrasonic dispersion not only increases the selectivity of CO_2 oxidation for CIs but also prevents the transformation of sp^2 carbon by non-oxidative destruction.

In summary, the most promising process is **P2**, which affords the lowest residual metal content, the most well-formed MWCNT structure with the fewest CIs, and a relatively high yield. As shown in Fig. 11, the dispersion

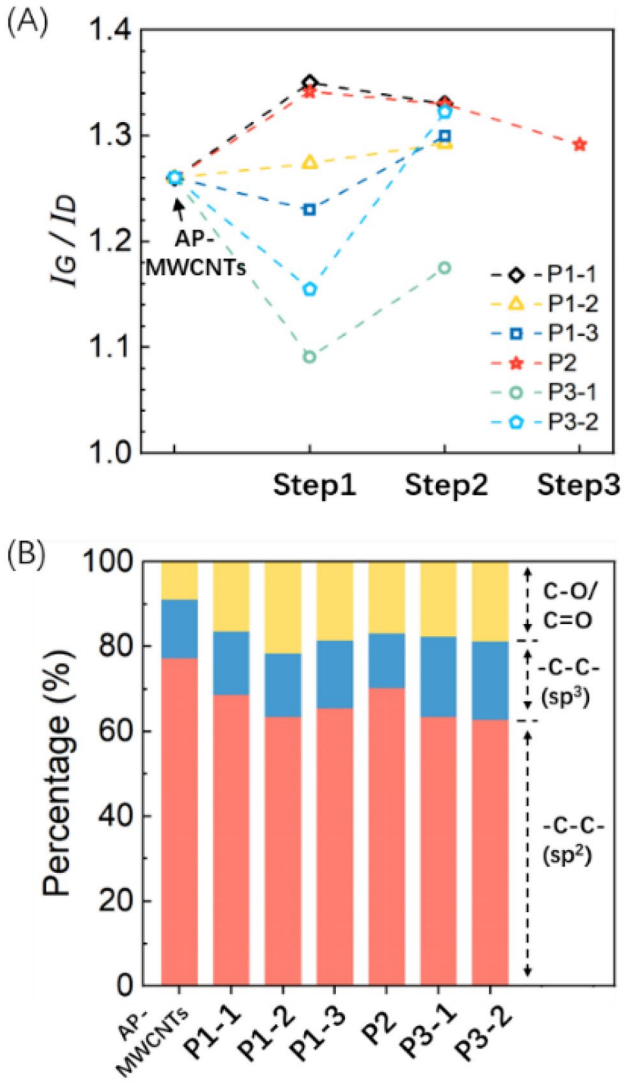

Fig. 10 **A** Raman results obtained after each step of various processes, **B** XPS results of CIs

operation in the first step is essential for separating CIs and even residual metal from the MWCNTs, exposing them and thus improving the effect of mild CO_2 oxidation and HCl non-oxidative etching. Consequently, the total yield of MWCNTs obtained by the CDM was 85.65 wt.%, and 87.20% of the residual metal was removed. The MWCNT yield and residual metal removal rate are 19.91% and 15.68% higher, respectively, than those obtained without the dispersion step (**P1-1**). This yield is also higher than those reported in the literature [1, 14] (79.2% for H_2, air oxidation, and HCl etching; 69.62% for air oxidation and HNO_3 and HCl etching). Most of the CIs were removed, and the MWCNT skeletons were preserved intact without notable damage. This mild three-step purification process for MWCNTs produced by CDM shows promise for large-scale industrial applications.

4 Conclusion

This work proposed a mild purification process based on the gas–solid and liquid–solid reaction dynamics for raw MWCNTs produced by CDM; this process exhibited increased selectivity of CO_2 gas phase oxidation, HCl liquid phase etching and a higher MWCNT yield.

A novel ultrasonic pretreatment method in ethanol was devised to separate and expose CIs and residual metal from MWCNTs, particularly those embedded within graphitic shells. This process effectively relieves mass transfer resistance encountered in the purification of AP-MWCNTs. The damage to MWCNTs depended on the operating temperature and duration of ultrasonication. The least damage to the MWCNT skeletons occurs, and only 2.5% of the sp^2 carbon is converted to sp^3 carbon, during 25 h of ultrasonic dispersion at 50 °C. CO_2 was used as a mild oxidant to remove CIs by the stepwise oxidation of carbon allotropes according to the thermodynamics, and HCl was used as an etching agent to remove residual metal because it causes the least damage to the MWCNT skeleton.

By combining the three operations into a cascade process, the purification of AP-MWCNTs was achieved, with a final one-way MWCNT yield of 85.65 wt.% and remaining residual metal content of 1.34 ± 0.06 wt.%. The MWCNT yield and residual metal removal rate were 19.91% and 15.68% higher, respectively, than those obtained without

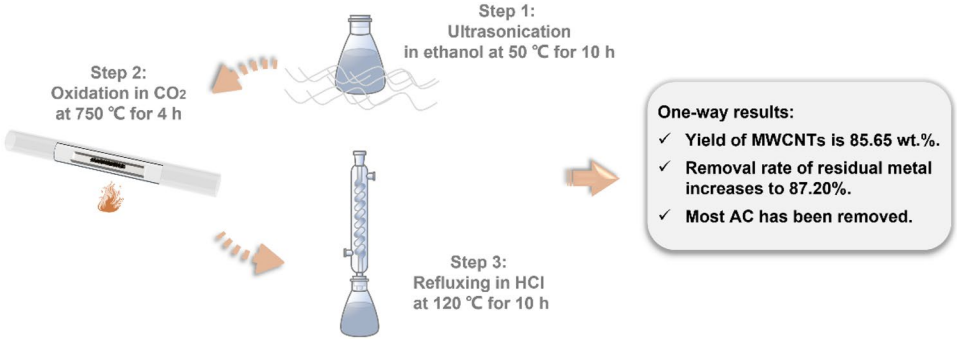

Fig. 11 Flow diagram of optimal process

ultrasonic dispersion. Moreover, this process prevents the conversion of sp^2 carbons by non-oxidative destruction, and the C–O/C = O content increased by only 8%.

This work describes an efficient method of disentangling raw MWCNTs; this mild purification process shows promise for application in qualified MWCNT production.

Supplementary Information The online version contains supplementary material available at https://doi.org/10.1007/s42823-023-00667-0.

Acknowledgements We appreciate the financial support from the National Natural Science Foundation of China (Grant No. 21978181 and 22178229). In addition, we would like to thank the Institute of New Energy and Low-Carbon Technology, Sichuan University, for SEM capture. Moreover, we are particularly grateful to the Center of Engineering Experimental Teaching, School of Chemical Engineering, Sichuan University, for TGA, FT-IR and Raman technical assistance.

Author contributions The manuscript was written through contributions of all authors. All authors have given approval to the final version of the manuscript. EC and QL conducted the experiments and characterizations, and PW, JH, CL, WJ gave supports on experiment guides and facilities.

Data availability All data generated or analyzed during this study are included in this published article.

Declarations

Conflict of interest The authors mentioned in this manuscript declare that they have no conflict of interest.

References

1. Ling X et al (2013) The effect of different order of purification treatments on the purity of multiwalled carbon nanotubes. Appl Surf Sci 276:159–166
2. Alshehri R et al (2016) Carbon nanotubes in biomedical applications: factors, mechanisms, and remedies of toxicity. J Med Chem 59:8149–8167
3. Tian TY et al (2023) Study on chitosan/carbon nanotubes modified materials used to enhance the performance of dental binder. Carbon Lett 33:1661–1667
4. Liu Q et al (2020) Catalytic decomposition of methane by two-step cascade catalytic process: simultaneous production of hydrogen and carbon nanotubes. Chem Eng Res Des 163:96–106
5. Qian JX et al (2020) Methane decomposition to produce CO -free hydrogen and nano-carbon over metal catalysts: a review. Int J Hydrogen Energy 45:7981–8001
6. Gupta N et al (2019) Carbon nanotubes: synthesis, properties and engineering applications. Carbon Lett 29:419–447
7. MacKenzie KJ et al (2010) An updated review of synthesis parameters and growth mechanisms for carbon nanotubes in fluidized beds. Ind Eng Chem Res 49:5323–5338
8. Goak JC et al (2019) Efficient gas-phase purification using chloroform for metal-free multi-walled carbon nanotubes. Carbon 148:258–266
9. Barkauskas J et al (2010) A novel purification method of carbon nanotubes by high-temperature treatment with tetrachloromethane. Sep Purif Technol 71(3):331–336
10. Ballesteros B et al (2008) Steam purification for the removal of graphitic shells coating catalytic particles and the shortening of single-walled carbon nanotubes. Small 4:1501–1506
11. Mercier, G et al (2013) Selective removal of metal impurities from single walled carbon nanotube samples. *New Journal of* Chemistry 37.
12. Suri A et al (2011) The superiority of air oxidation over liquid-phase oxidative treatment in the purification of carbon nanotubes. Carbon 49:3031–3038
13. Clancy AJ et al (2016) Systematic comparison of conventional and reductive single-walled carbon nanotube purifications. Carbon 108:423–432
14. Li QL et al (2008) Removal of metal catalyst in multi-walled carbon nanotubes with combination of air and hydrogen annealing followed by acid treatment. J Nanosci Nanotechnol 8:5807–5812
15. Lin Y et al (2015) Purification of carbon nanotube sheets. Adv Eng Mater 17(5):674–688
16. Wang D et al (2018) CO2 oxidation of carbon nanotubes for lithium-sulfur batteries with improved electrochemical performance. Carbon 132:370–379
17. Vaisman L et al (2006) The role of surfactants in dispersion of carbon nanotubes. Adv Coll Interface Sci 128–130:37–46
18. Montazeri A et al (2011) The effect of sonication time and dispersing medium on the mechanical properties of multiwalled carbon nanotube (MWCNT)/epoxy composite. Int J Polym Anal Charact 16(7):465–476
19. Montazeri A et al (2014) Effect of sonication parameters on the mechanical properties of multi-walled carbon nanotube/epoxy composites. Mater Des 56:500–508
20. Lu KL et al (1996) Mechanical damage of carbon nanotubes by ultrasound. Carbon 34(6):814–816
21. Suave J et al (2009) Effect of sonication on thermo-mechanical properties of epoxy nanocomposites with carboxylated-SWNT. Mater Sci Eng, A 509(1–2):57–62
22. Fatemi SM et al (2015) Recent developments concerning the dispersion of carbon nanotubes in surfactant/polymer systems by MD simulation. Journal of Nanostructure in Chemistry 6(1):29–40
23. Cui, H et al (2017) Effects of Various Surfactants on the Dispersion of MWCNTs–OH in Aqueous Solution. Nanomaterials 7 (9).
24. Liu, Q et al (2022) NiFe/Al2O3/Fe-frame catalyst for COx-free hydrogen evolution from catalytic decomposition of methane: Performance and kinetics. Chemical Engineering Journal *436*.
25. Lehman JH et al (2011) Evaluating the characteristics of multiwall carbon nanotubes. Carbon 49(8):2581–2602
26. Dunens OM et al (2009) Synthesis of multiwalled carbon nanotubes on Fly ash derived catalysts. Environ Sci Technol 43(20):7889–7894
27. Lima A et al (2009) Purity evaluation and influence of carbon nanotube on carbon nanotube/graphite thermal stability. J Therm Anal Calorim 97(1):257–263
28. Nuernberg GDB et al (2011) Methane conversion to hydrogen and nanotubes on Pt/Ni catalysts supported over spinel MgAl2O4. Catal Today 176(1):465–469
29. Fang W et al (2014) Hydrogen production from bioethanol catalyzed by NiXMg2AlOY ex-hydrotalcite catalysts. Appl Catal B 152–153:370–382
30. Azhari, S et al (2018) A better understanding of CNTs chemical purification and functionalization processes, 13th IEEE International Conference on Semiconductor Electronics (IEEE ICSE), Kuala Lumpur, MALAYSIA, Aug 15–17; Ieee: Kuala Lumpur, MALAYSIA, 25–28.
31. McKee GSB et al (2009) Dimensional control of multi-walled carbon nanotubes in floating-catalyst CVD synthesis. Carbon 47(8):2085–2094

32. Cho HG et al (2009) A simple and highly effective process for the purification of single-walled carbon nanotubes synthesized with arc-discharge. Carbon 47(15):3544–3549
33. Hou PX et al (2001) Purification of single-walled carbon nanotubes synthesized by the hydrogen arc-discharge method. J Mater Res 16(9):2526–2529
34. He RUI, et al (2013) Effects of Ultrasonic Radiation Intensity on the Oxidation of Single-Walled Carbon Nanotubes in a Mixture of Sulfuric and Nitric Acids. Nano 08 (04).
35. Rahmanian S et al (2013) Synthesis of vertically aligned carbon nanotubes on carbon fiber. Appl Surf Sci 271:424–428
36. Krause B et al (2010) Dispersability and particle size distribution of CNTs in an aqueous surfactant dispersion as a function of ultrasonic treatment time. Carbon 48(10):2746–2754
37. Rastegarpanah A et al (2019) Influence of group VIB metals on activity of the Ni/MgO catalysts for methane decomposition. Appl Catal B 248:515–525
38. Liu C et al (1999) Hydrogen storage in single-walled carbon nanotubes at room temperature. Science 286(5442):1127–1129
39. Verdejo R et al (2007) Removal of oxidation debris from multi-walled carbon nanotubes. Chem Commun 5:513–515
40. Zhang L et al (2011) Mild hydrothermal treatment to prepare highly dispersed multi-walled carbon nanotubes. Appl Surf Sci 257:1845–1849
41. Wang YH et al (2007) A highly selective, one-pot purification method for single-walled carbon nanotubes. J Phys Chem B 111(6):1249–1252
42. Edwards ER et al (2011) Evaluation of residual iron in carbon nanotubes purified by acid treatments. Appl Surf Sci 258(2):641–648
43. Wepasnick KA et al (2011) Surface and structural characterization of multi-walled carbon nanotubes following different oxidative treatments. Carbon 49(1):24–36
44. Das R et al (2014) Common wet chemical agents for purifying multiwalled carbon nanotubes. J Nanomater 2014:1–9